CEAS Aeronautical Journal
https://doi.org/10.1007/s13272-024-00776-0

ORIGINAL PAPER

Turbine cooling air estimation in thermodynamic simulations

Björn Schneider[1]

Received: 19 February 2024 / Revised: 16 September 2024 / Accepted: 23 September 2024

Abstract
Modern gas turbines utilize a high amount of the core mass flow rate for component cooling. Thus, a coherent thermodynamic gas turbine representation demands a well-modeled secondary air system, which is able to estimate mass flow rates depending on respective design decisions. In this paper, the focus is set on the estimation of turbine blade cooling air. For this purpose, five different methods are presented and analyzed. The described concepts can be split into empirical and semi-empirical approaches. The semi-empirical approaches, the Horlock [1], Jonsson [2] and the Halliwell [3] method, are able to predict the blade temperature based on a given cooling mass flow rate or the needed cooling air based on a given blade temperature. In contrast, the empirical methods, the Grieb [4] and the Walsh [5] method, can only predict the cooling air consumption. Due to the fully empirical approaches the field of application is limited to the considered engine structures. On the other hand, the empirical methods lead to a better convergence behavior in comparison to the semi-empirical approaches due to their relatively simple calculation methods. The selected cooling air estimations are implemented in the performance code DLRp2 [6–8]. Therefore, processes and methods are deployed that allow to estimate turbines with unlimited cooled stages. Additionally, an off-design procedure is proposed to consider the occurring stagnation temperature drop between stator and rotor based on a reference temperature offset. A simplified thermodynamic gas turbine model is used to analyze the different cooling air estimation methods. For this purpose, sensitivity analyses for the main cooling air parameters are carried out. Moreover, all methods that were developed for the most stressed operating point are compared. Finally, the simplified model is calibrated to NASA's energy efficient engine [9].

Keywords Cooling air estimation · Thermodynamic engine simulation · Blade temperature prediction · Secondary air system · Gas turbine design

1 Introduction

Nowadays, the rising pressure and temperature levels of gas turbines leads to increasing demands on hot section components of gas turbines. Beside the application of new materials and manufacturer processes a growing ratio of the core mass flow rate is used for the turbine cooling. Modern aircraft engines may take 20% to 25% of the high-pressure compressor mass flow as cooling air for the turbine stages [10]. Consequently, the amount of cooling air has an impact on the overall engine performance and therefore the cooling air should already be considered in early design stages of gas turbine.

This paper deals with an overview of published cooling air prediction methods by discussing five prominent approaches that are suitable for thermodynamic simulations: Grieb [4], Walsh [5], Horlock [1], Jonsson [2] and Halliwell [3] (see Sect. 2). The selected methods are implemented in the DLR in-house developed performance code DLRp2 [6–8]. The evolved computational logic, the required method adaptions and improvements are presented and discussed. Finally, a simplified gas turbine model is used to compare the methods and calibrate them to the high-pressure turbine (HPT) of NASA's energy-efficient engine.

✉ Björn Schneider
bjoern.schneider@dlr.de

[1] Institute of Propulsion Technology, German Aerospace Center (DLR), Linder Höhe, Cologne 51147, NRW, Germany

Published online: 13 November 2024

2 Cooling air estimation methods

In this section, the considered cooling air estimation methods are briefly described. All presented methods are able to predict the required cooling mass flow rates without a detailed knowledge of the considered engine and are therefore generally applicable within performance simulations.

The methods from Grieb [4] and Walsh [5] are fully empirical and correlate the coolant mass flow rate to representative fluid temperatures. Both estimations are based on existing engine data and thus these correlations should not be used for novel engine structures. At this point, it should be noted that the engines database for the Grieb method includes values for entry into service from 1970 up to 2000 and that the used engine data for the Walsh method are not published.

The semi-empirical methods are adapted from Horlock [1], Jonsson [2] and Halliwell [3]. These methods assume, that the blades can be seen as plate heat exchangers that are calculated with Eq. 1.

$$\begin{aligned}\dot{Q} &= \underbrace{w_c \cdot C_{p-c} \cdot \left(T_{c-out} - T_{c-in}\right)}_{\text{coolant}} \\ &= \underbrace{w_g \cdot C_{p-g} \cdot \left(T_{g-out} - T_{g-in}\right)}_{\text{hot gas}} \\ &= \underbrace{h_g \cdot A_b \cdot \left(T_{g-in} - T_b\right)}_{\text{blade}}\end{aligned} \tag{1}$$

The heat flow $\dot{Q}$ is determined in simplified form via the enthalpy change of the cooling air mass flow rate w_c or the enthalpy change of the hot gas flow rate w_g, whereby the process can also be described on the base of the heat transfer within the blade in that a representative blade area A_b and a heat transfer coefficient on the hot gas side h_g is used.

2.1 Grieb [4]

For the Grieb method a correlation between the turbine cooling air consumption w_c and the reference temperature T_{ref} is created on the base of realized engine data. Figure 1 shows the stage coolant mass flow rate divided by the compressor mass flow rate in front of the coolant extraction position w_{comp} in dependency of the reference temperature T_{ref}, which is determined with the stator outlet temperature (SOT) of the considered stage and the coolant temperature T_c. The split between the stator and rotor cooling airflow is estimated with the help of Fig. 2. This chart shows the ratio of the rotor cooling mass flow rate to the compressor mass flow rate in front of the coolant extraction position over the reference temperature.

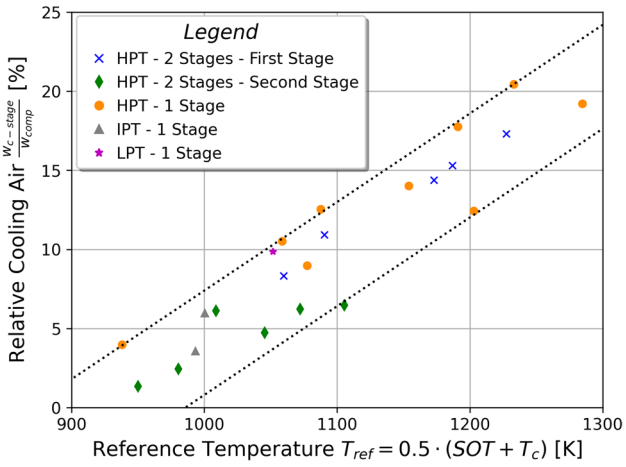

Fig. 1 Stage cooling air mass flow rate (based on [4, Chart 5.2.3.16])

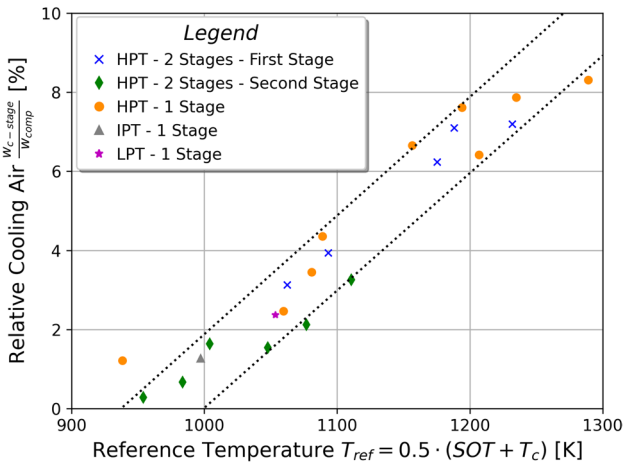

Fig. 2 Rotor cooling mass flow rate (based on [4, Chart 5.2.3.17])

The cooling air estimation should be applied at maximum take-off (MTO) at an altitude of zero and a temperature offset to international standard atmosphere of zero.

2.2 Walsh [5]

The method from Walsh correlates the coolant mass flow rate w_c divided by the overall gas turbine inlet mass flow rate w_{engine} with the SOT of the considered turbine stage (see Fig. 3). It should be noticed that the Walsh method has to be applied at cruise (CR) for aircraft engines and at base load for power gas turbines.

2.3 Horlock [1]

The Horlock calculation assumes that the blades can be approximated by simple plate heat exchangers. For this

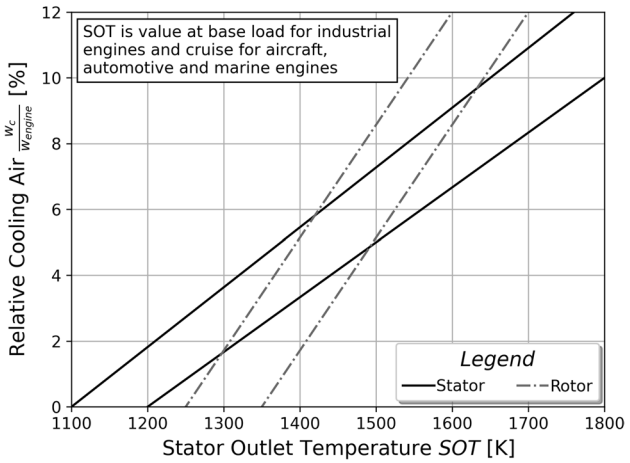

Fig. 3 Stage and rotor cooling mass flow rate (based on [5, Chart 5.16])

purpose, an initial blade geometry must be estimated, which is summarized in the C_{std} parameter (see Eqs. 2 and 3). The area ratio λ_H equals the blade surface area A_{sg} divided by the throat area A_{xg}. This area ratio can be approximated by the blade cord length c, the spacing between the blades (pitch) bs and the discharge angle α. The area ratio λ_H is then summarized with the heat capacity ratio of the hot gas C_{p-g} and the coolant C_{p-c} to the variable C_{lam}. This variable multiplied by the averaged Stanton number of the hot gas St_g results in the value C_{std}, which can be seen as a technology factor and should be corrected by a safety factor S_f to get more realistic results (see Eq. 4). Low values of C_{std} represent high technology levels.

$$C_{std} = \underbrace{\lambda_H \cdot \frac{C_{p-g}}{C_{p-c}}}_{C_{lam}} \cdot \underbrace{\frac{h_g}{c_g \cdot \varrho_g \cdot C_{p-g}}}_{St_g} = C_{lam} \cdot St_g \tag{2}$$

$$\lambda_H = \frac{A_{xg}}{A_{sg}} = \frac{2 \cdot L \cdot c}{L \cdot bs \cdot \cos(\alpha)} = \frac{2 \cdot c}{bs \cdot \cos(\alpha)} \approx 10 \tag{3}$$

$$C = C_{std} \cdot S_f \tag{4}$$

Beside the geometrical description, a definition of the heat flux is necessary. For this, the cooling efficiency η_c and the overall cooling effectiveness ε_0 is used (see Eq. 5). The cooling efficiency is a measure of the inner blade heat exchange. A high value means that the coolant outlet temperature T_{c-out} approximates the blade temperature T_b. The overall cooling effectiveness is calculated with the blade temperature T_b, the gas inlet temperature T_{g-in} and the cooling inlet temperature T_{c-in}. This overall effectiveness can also be seen as a further technology factor.

$$\begin{aligned} \eta_c &= \frac{T_{c-out} - T_{c-in}}{T_b - T_{c-in}} \\ \varepsilon_0 &= \frac{T_{g-in} - T_b}{T_{g-in} - T_{c-in}} \end{aligned} \tag{5}$$

Moreover, the Horlock method provides different mathematical approaches for the cooling air mass prediction depending on the used blade cooling type. In these models the cooling air ratio ζ is defined by the ratio of the cooling mass flow rate w_c and the blade raw inlet gas mass flow rate w_g (see Eq. 6).

$$\zeta = \frac{w_c}{w_g} \tag{6}$$

2.3.1 Convective cooling

For convective cooled blades the cooling air ratio ζ is calculated by equation 7. For this cooling estimation besides the technology factors C and ε_0, the inner heat flux is considered by the cooling efficiency η_c.

$$\zeta = \frac{w_c}{w_g} = \frac{K \cdot \varepsilon_0}{1 - \varepsilon_0} \quad \text{with} \quad K = \frac{C}{\eta_c} \tag{7}$$

2.3.2 Convective and film cooling

For the calculation of a film-cooled blade row a further parameter has to be defined, the film cooling effectiveness ε_f (see equation 8). This parameter describes how effective the coolant is shielding the blade from the surrounding gas. The determination of this value is difficult because the adiabatic blade wall temperature T_{aw} is typically not known.

$$\varepsilon_f = \frac{T_{g-in} - T_{aw}}{T_{g-in} - T_{c-out}} \tag{8}$$

Equation 9 shows in which way the cooling air mass flow ratio is determined.

$$\zeta = \frac{w_c}{w_g} = C \cdot \frac{\varepsilon_0 - (1 - \eta_c) \cdot \varepsilon_f - \varepsilon_0 \cdot \varepsilon_f \cdot \eta_c}{\eta_c (1 - \epsilon_0)} \tag{9}$$

This method can also be extended for the consideration of thermal barrier coatings [11]. The extended approach requires detailed knowledge about the used coating. This knowledge is usually not available during a thermodynamic simulation and thus it is not described in detail here.

2.4 Jonsson [2]

The Jonsson method is based also on the heat flux calculation Eq. 1 and the variables are reduced in a similar way to the Horlock method. For the Jonsson method the geometrical parameter λ_H describes the blade geometry as shown in Eq. 3. This parameter is combined with the Stanton number and the cooling efficiency to the variable b as shown in Eq. 10.

$$\frac{w_c \cdot C_{p-c}}{\dot{w}_g \cdot C_{p-g}} = \zeta \cdot \frac{C_{p-c}}{C_{p-g}} = b \cdot \left(\frac{T_{g-in} - T_b}{T_b - T_c} \right)^s \quad b = \frac{\lambda_H \cdot St_g}{\eta_c} \tag{10}$$

The required cooling efficiency η_c is determined by Eq. 11. It should be noted that the cooling efficiency for film cooled blades $\eta_c = \eta_{c-film}$ is smaller than the convective cooling efficiency $\eta_c = \eta_{c-conv}$ because the blade temperatures for cooled blades T_b are smaller than the inlet gas temperatures T_{g-in}. In order to offset this phenomenon, the exponent s can be modified according to the type of cooling.

$$\begin{aligned} \eta_{c-conv} &= \frac{T_{c-out} - T_{c-in}}{T_b - T_{c-in}} \\ \eta_{c-film} &= \frac{T_{c-out} - T_{c-in}}{T_{g-in} - T_{c-in}} \end{aligned} \tag{11}$$

Thus, the parameter b for convective cooled blades corresponds to the Horlock parameter K with a safety factor of $S_f = 1$ and can also be regarded as a technology factor. The exponent s represents the blade cooling type. For convective cooling, the value should be set to one and for film-cooled blades s should be set in the range from one to two. The Jonsson method can be used for the prediction of cooling air and blade temperature for every blade row [12] as well as for the estimation of turbines stages [2]. The stage consideration allows calculations without the information of row-based gas properties and also lowers the numerical effort. But this simplification also leads to a reduction of information.

2.5 Halliwell [3]

The Halliwell method determines the overall cooling effectiveness ε_0 by an empirical correlation that is given by Eq. 12.

$$\begin{aligned} \varepsilon_0 &= \frac{\zeta}{\zeta + C_1} = \frac{T_{g-in} - T_b}{T_{g-in} - T_{c-in}} \\ T_b &= T_{g-in} - \varepsilon_0 \cdot \left(T_{g-in} - T_{c-in} \right) \end{aligned} \tag{12}$$

It should be noted that Eq. 12 describes the same relationship as Eq. 7 for convective cooled blades of the Horlock method, except for the variable name K that is replaced with C_1. The main difference between the approaches is that Halliwell uses Eq. 12 for all blade cooling types. Typically, the range for the technology factor C_1 is set from 0.03 to 0.07, whereby low values represent a higher technology level. In [3] is also mentioned that the temperature reduction that results from the transition from absolute to relative coordinate system between the stator and the rotor can be considered by multiplying the gas temperature T_{g-in} by the factor 0.9.

3 Implementation

Some assumptions, simplifications and extensions were necessary for the application of the cooling air methods within thermodynamic computations.

3.1 Grieb

The Grieb diagrams in Sect. 2 return for a given reference temperature a wide range of possible cooling mass flow rates. For thermodynamic calculations, a single value has to be estimated. Thus, an auxiliary value ϕ is introduced. This value describes the relative position between the two border curves. The lower curve is defined as $\phi = 0$ and the upper curve as $\phi = 1$. The required curves are implemented with the calculation logic that is given in Eq. 13. This implementation avoids negative cooling mass flow rates and uses the auxiliary value ϕ as a parameter that represents the cooling technology level (lower values equal higher technology levels). The derived functions from the graphs in Sect. 2.1 are given in Eq. 14 for the determination of the stage cooling air and Eq. 15 for estimation of the rotor cooling air.

$$\frac{w_c}{w_{comp}} = \max\left(F_0 + \phi \cdot \left(F_1 - F_0\right);\ 0\right) \tag{13}$$

$$\begin{aligned} F_{0-stage} &= \left(0.056 \cdot T_{ref} - 55.3\right) \cdot 10^{-2} \\ F_{1-stage} &= \left(0.056 \cdot T_{ref} - 48.605\right) \cdot 10^{-2} \end{aligned} \tag{14}$$

$$\begin{aligned} F_{0-rot} &= \left(0.03 \cdot T_{ref} - 29.684\right) \cdot 10^{-2} \\ F_{1-rot} &= \left(0.03 \cdot T_{ref} - 28.12\right) \cdot 10^{-2} \end{aligned} \tag{15}$$

For the rotor cooling air estimation, the technology factor can be different to the stage technology factor ϕ. Consequently, a second parameter ϕ_{rot} is introduced. This factor also influences the stator coolant consumption and thus the reference temperature T_{ref}. As an example, a reduced ϕ_{rot} shifts the cooling air mass flow rate from the rotor to stator. This reduces the reference temperature T_{ref} and thus the required stage cooling mass flow rate.

To avoid the second technology parameter ϕ_{rot}, a balancing function was created and implemented that correlates the stator-rotor coolant split in dependency of the reference temperature T_{ref}. For this purpose, the given gas

turbines are assigned in Fig. 1 and 2. The resulting engine data sets are used to determine a rotor cooling ratio $\frac{w_{c-stage}}{w_{c-rot}}$. Afterwards, separate linear balance functions for the first and second stage are created by considering all data for two-stage HPT's. The point of intersection of the balance functions is located at a reference temperature of 1072 K which is used to change the applied balance function. Additionally, a lower split boundary is set to 2.1 which is reached at a reference temperature of 1263 K. This boundary ensures that the rotor cooling mass flow rate is smaller than the stator cooling mass flow rate which can be seen as the usual case in existing engines [9, 10, 13, 14]. Figure 4 shows the described cooling ratio over the reference temperature with the resulting overall balancing function (Eq. 16).

$$\begin{aligned}
\frac{w_{c-stage}}{w_{c-rot}} &= \begin{cases} F_{b-0} & T_{ref} \leq 1072.1\,\mathrm{K} \\ F_{b-1} & \text{if} \quad T_{ref} \leq 1262.89\,\mathrm{K} \\ F_{b-2} & T_{ref} > 1262.89\,\mathrm{K} \end{cases} \\
F_{b-0} &= -0.0151 \cdot T_{ref} + 18.842 \\
F_{b-1} &= \frac{29}{10^4} \cdot (1072.1 - T_{ref}) + F_{b-0}(1072.1) \\
F_{b-2} &= const = F_{b-1}(1262.89) = 2.1
\end{aligned} \tag{16}$$

Additionally, some simplified calculation methods are implemented, that can improve the convergence behavior, reduce the complexity and can be used to evaluate initial system values. For example, the coolant stator-rotor-split can be set directly and it is also possible to use the stage inlet temperature instead of the SOT for the reference temperature calculation. Moreover, the turbine inlet mass flow rate can be used as the reference mass flow rate.

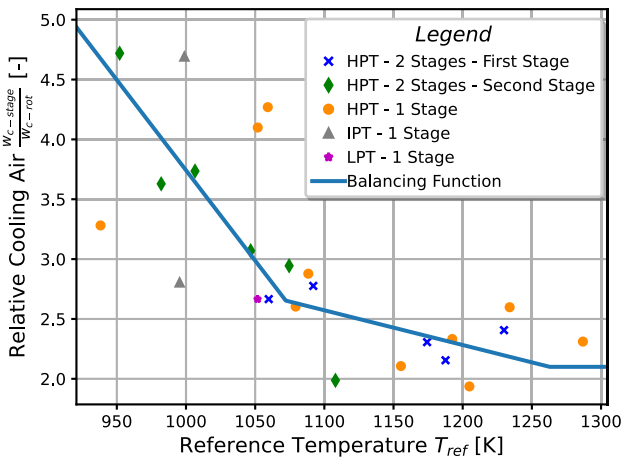

Fig. 4 Balancing function for the rotor-stator cooling air split

3.2 Walsh

The Walsh diagram provides a range of cooling air mass flow rates for a given SOT. Therefore, an auxiliary value ϕ is implemented to describe the relative position between the linear functions, similar to the Grieb method (see Sect. 3.1). In Fig. 3 are no more information given that allows an improved assignment between the stator and rotor cooling mass flow rates. Thus, for both determination the same auxiliary value ϕ is applied. The curves from the graph are implemented in the performance code by using the functions in Eq. 17 for the stator and the functions in Eq. 18 for the rotor by using the logic from Eq. 13.

$$\begin{aligned}
F_{0-stat} &= \left(\frac{SOT}{60} - 20\right) \cdot 10^{-2} \\
F_{1-stat} &= \left(\frac{SOT}{55} - 20\right) \cdot 10^{-2}
\end{aligned} \tag{17}$$

$$\begin{aligned}
F_{0-rot} &= \left(\frac{SOT \cdot 12}{350} - \frac{150}{350}\right) \cdot 10^{-2} \\
F_{1-rot} &= \left(\frac{SOT \cdot 12}{350} - \frac{162}{350}\right) \cdot 10^{-2}
\end{aligned} \tag{18}$$

3.3 Horlock

In many cases, the required detailed design information for the Horlock method is not available. Especially, the heat transfer coefficient cannot be determined without detailed knowledge of the gas flow and blade design [15]. Hence, [1] recommends to use C_{lam} as a constant variable that should be set to 20 for state-of-the-art gas turbines and the Stanton number to $1.5 \cdot 10^{-3}$. Additionally, [11] recommends to set the safety factor to 1.5 which makes the value $C = 0.045$. It is also suggested that the cooling efficiency η_c can be approximated with 0.7 and the film cooling effectiveness ε_f with 0.4. As a result, the Horlock cooling estimation for thermodynamic calculations considers less free parameter as the theoretical derivation pretends. For the consideration of different technology levels, the cooling efficiency η_c and the film cooling effectiveness ε_f can be varied. It should be noted that the coefficient C_{std} must be adapted if cycles with higher changes in the fluid properties are carried out. For example, Cheng-cycles or cycles with untypical gas temperatures can lead to not negligible changes in the heat capacity ratio and the Stanton number (see Eq. 2). In [1] it is pointed out, that the influence of the fluid properties has to be considered for gas temperatures outside the range from 1500 K to 2200 K. Hence, the fluid property changes have not been implemented for the C_{std} so far.

In summary, the Horlock method input parameters can be reduced to C_{std}, S_f, ε_f, η_c and T_b for thermodynamic computations.

3.4 Jonsson

The Jonsson method is based on the same physical approach as the Horlock method. The main difference is that the Jonsson method is already adjusted for thermodynamic simulations by eliminating geometrical and detailed heat flux information.

Table 1 gives an overview of design parameters which are suggested in literature. In the upper part the Jonsson parameter b for overall stage considerations [2] and in the part below the values for row-based simulations are given [12]. At the bottom of the table the suggested range of the Jonsson exponent s can be found.

It should also be noted that in [2] the design parameters were fitted to a realized stationary gas turbine. The optimization of the design parameter results in $s = 1$ and $b = 0.1884$ for the considered film-cooled gas turbine. This example shows the s parameter can be varied in the whole range for film-cooled engines. Thus, in the following sections the averaged value of $s = 1.5$ is used as default value.

3.5 Halliwell

For the Halliwell method the overall cooling effectiveness has to be calculated. Therefore, the Eq. 12 can be used with an assumed C_1 value, which is typically in the range from 0.03, for sophisticated multi-pass configurations with film cooling, up to 0.07, for blades with simple radial holes. For calculations without any further information, the mean value of 0.05 should be used [3].

3.6 Temperature drop between stator and rotor

In an uncooled turbine stage under equilibrium conditions, the airfoil temperature corresponds approximately to the stagnation temperature of the fluid. This temperature equals for stators the total fluid temperature. For rotating blades, the stagnation temperature depends on the rotor velocity and thus on the radius and the rotational speed. Equation 19 describes how the stagnation temperature T_{stag} is calculated for a swirl free flow. Generally, the turbine absolute fluid velocity c at the stator is bigger than the relative velocity w at the rotor due to the circumferential speed that occurs in a fixed direction of rotation [4, 13]. If a constant static temperature T and heat capacity C_p are considered, a reduced stagnation temperature results for the rotor.

$$\begin{aligned} \text{Stator: } T_{stag} &= T + \frac{c^2}{2 \cdot C_p} \\ \text{Rotor: } T_{stag} &= T + \frac{w^2}{2 \cdot C_p} \end{aligned} \tag{19}$$

The detailed information about the fluid properties and blade geometries are typically unknown during thermodynamic analyses. Thus, a simplified method is developed. Equation 20 shows the created approach which neglects the impact of blade radius changes from hub to tip. This simplification can be justified by the fact that typically only the first turbine stages are cooled and the first blades have usually small heights. Moreover, a constant reaction ratio φ_{hM} is assumed for all operating points. During thermodynamic calculations a design temperature offset can be defined or a selected default value off $\Delta T = -100\,\text{K}$ [13] is used, which can be seen as a conservative assumption. Then the given

Table 1 Jonsson design parameters adapted from [2, 12]

Parameter	Cooling	Stages	Suggested
b	Convective	One	0.10 ...0.30
		Two	0.20 ...0.70
		Less conservative	
		One	0.10 ...0.20
		Two	0.10 ...0.30
	Film	One	0.05 ...0.10
		Two	0.10 ...0.20
Parameter	Cooling	Row	Suggested
b	Film	Stator	0.06
		Rotor	0.05
Parameter	Cooling		Suggested
s	Convective		1
	Film		1 ...2

design value is corrected in off-design calculations by the current spool speed.

$$\Delta T = \frac{u^2}{2 \cdot C_p} \cdot \left(3 - 4 \cdot \varphi_{hM}\right) \propto n^2$$
$$\Rightarrow \Delta T_{off-design} = \Delta T_{design} \cdot \left(\frac{n}{n_{design}}\right)^2 \tag{20}$$

3.7 Performance coupling

In the used performance code DLRp2, the computation is divided into design point and off-design point calculations. During a design run extended performance component information is required for a full description, e.g. the design pressure ratio. Hence, the design calculation is typically carried out for the best-known operating point. Afterwards, off-design calculations can be executed, whereby the changed conditions are considered using functionalities that determines the current behavior on the base of the design values.

In this section the components are presented which have a direct impact on the cooling air computation: the already implemented *turbine* and the newly created *cooling air computation*.

3.7.1 Turbine

In design calculations, the turbine requires an efficiency, a relative reduced spool speed, a turbine characteristic and a speed line position as input. In a first step, the turbine pressure ratio is determined by the inlet fluid conditions, the efficiency and the power that is required by the connected shaft. Afterwards, the extended data set is used to scale the turbine characteristic to the current design conditions.

During off-design calculations the mechanical shaft speed, the required shaft power and the inlet fluid conditions are known. These values lead to a unique position in the characteristic from which the efficiency and the pressure ratio can be derived. A detailed description of this process can be found in [10].

Additionally, the turbine representation enables the connection of cooling air through four ports. These ports are represented by yellow triangles (see Fig. 5). The first and second port, can be seen as cooling air that is injected up- and downstream of the stator. In other words, the injected coolant takes part in the energy conversion of the turbine. The third and fourth connections represent cooling air injections around the power extraction. Thus, the third connection is also taking part on the turbine power balance. According to this, the three cooling ports are mixed with the main fluid before the turbine computation is called. Then the cooling air from the fourth port is mixed with the expanded fluid. This turbine implementation allows to simulate multi-stage turbines with a freely selectable stator outlet temperature and the possibility to exclude cooling streams from power extraction [5].

3.7.2 Cooling air computation

The current turbine computation cannot provide the needed information for the considered cooling air methods (see Sect. 2). Moreover, the turbine representation only allows a restricted number of cooling air connections and turbine stages. Consequently, a new method has been implemented that determines the required values for an unrestricted amount of turbine stages in a post process of the model computation.

In the created method the outlet conditions of all considered turbine sections are calculated in two steps. The first one computes the fluid conditions based on the power extraction. Then in a second step, the defined cooling air mass flow rate is mixed with the main fluid. Depending on the chosen cooling air estimation mode the turbine section can be a row, a stage or a whole turbine. At this point, it should be noted that in stator rows no power extraction occurs and thus only the second calculation step is necessary. As described in Sect. 3.7.1 the current turbine implementation cannot provide fluid information for intermediate positions of multi-staged turbines. For the following computations, a simple approach is used that approximates stage power extraction by dividing the overall turbine enthalpy equally between the stages.

The calculation method is carried out after the thermodynamic calculation so that the required model information is

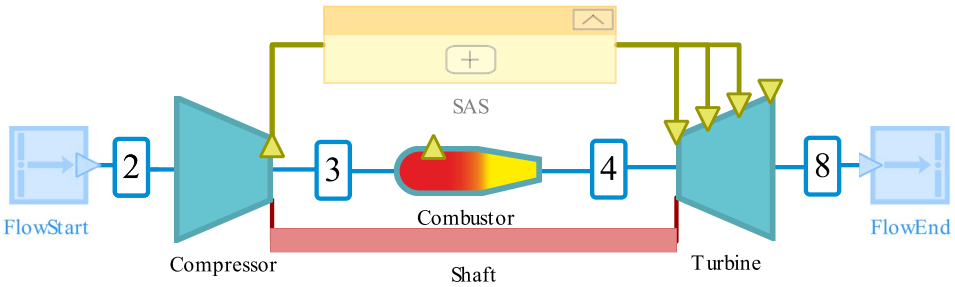

Fig. 5 Simplified gas turbine performance model

available in full. The implementation as a post process leads to the disadvantage that the results have no direct influence on the thermodynamic model. Thus, the calculated cooling air must be fed back after the model computation. This procedure is repeated until the deviation is under a certain limit. For this purpose, the performance code already provides a non-linear solver that enables the user to define parameters that should be matched by adjusting model input values [16].

4 Method analysis

In this section, the behavior of the cooling air methods is investigated. Therefore, a simplified performance model of a gas turbine is set up and presented in Sect. 4.1. Then the model is used to carry out sensitivity studies for the cooling methods. Moreover, some further relations between the methods are derived and discussed in Sect. 4.2. Finally, the methods are compared to each other in Sect. 4.3 and the input parameter for the cooling air methods are calibrated in Sect. 4.4.

4.1 Thermodynamic model

For the following analyses, a simple gas turbine model is used which is shown in Fig. 5. In this model, the extracted turbine power is used to drive the connected compressor. Table 2 shows the chosen main design values. The tapping point for the cooling air of the first turbine stage is connected to the compressor outlet. The pressure drop that results from the energy extraction of the first stage allows a reduced cooling air pressure level for the cooling air of the following stages. Hence the second stage is cooled with cooling air that is extracted from an intermediate point of the compressor. In the current model, the relative compressor enthalpy for the tapping point of the second stage is set to 70%.

In the following studies, the calculated cooling air is not fed back into the model. As a result, the necessary cooling mass flow rates are not influenced by side effects from the turbo components and the design parameter from table 2 are constant. The stagnation temperature offset for the row-based methods is set to -100 K (see Sect. 3.6) and the maximum allowable blade temperature T_b is set to 1250 K [4].

4.2 Main parameter influence

All cooling air methods provide technology factors that must be defined. In this section the influence of the main parameters is investigated.

4.2.1 Grieb

The Grieb method provides two design parameters, the technology factor and the rotor-stator cooling air split. It should be noted that a detailed analysis of the technology factor is not necessary because for the used model the influence is similar to already presented Fig. 1.

Fig. 6 shows the influence of the split factor $w_{c-rot}/w_{c-stage}$ on the estimated cooling mass flow rate for a constant turbine inlet temperature (TIT) of 1800 K and a stage technology factor ϕ of 0.5. It can be seen that the split factor has an influence on the total amount of cooling air. The cooling air amount rises with an increasing split factor (also see table 3). This dependency results from the influence of the split factor on the SOT and thus on the reference temperature T_{ref} (see Sect. 2.1). For the chosen boundary conditions the split factor can change the resulting cooling air amount by

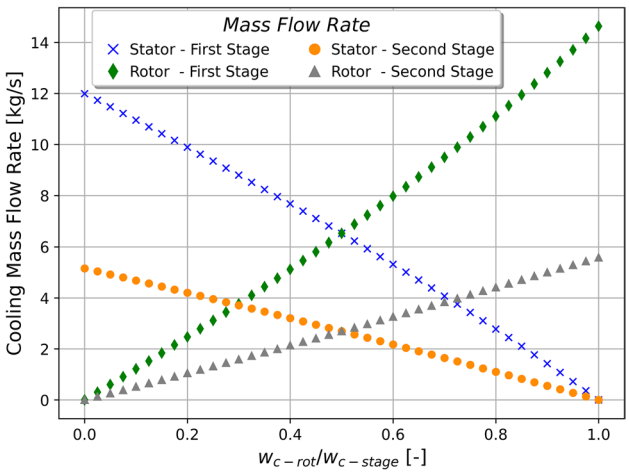

Fig. 6 Influence of the cooling air split between rotor and stator on the cooling mass flow rate

Table 2 Design conditions of the simplified gas turbine model

Position	Parameter	Unit	Value
2	Mass Flow Rate	[kg/s]	67,26
	Temperature	[K]	303.15
	Pressure	[bar]	1.013
3	Temperature	[K]	900
	Pressure	[bar]	34.346

Table 3 Selected results from split factor study

$w_{c-rot}/w_{c-stage}$		[-]	0.0	0.5	1.0
Stage 1	*SOT*	[K]	1643	1705	1800
	w_c	[kg/s]	11.99	13.02	14.63
Stage 2	*SOT*	[K]	1399	1411	1422
	w_c	[kg/s]	5.16	5.39	5.58
Stage 1 & 2	w_c	[kg/s]	17.14	18.41	20.21

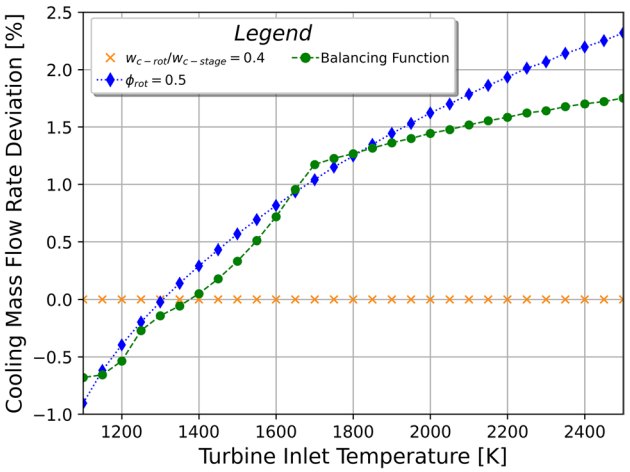

Fig. 7 Influence of the stage cooling air split mode

$\frac{20.21-17.14}{18.41} \approx 16.7\%$, whereby the technology factor ϕ influences the cooling air amount with the same variation by roughly 7%.

To quantify the influence of the selected prediction method of the split factor in Fig. 7 a comparison of the available functions is shown. The plot shows the percentage deviation of the predicted mass flow rates related to the mass flow rate of a fixed split factor of 0.4 for different TIT. This comparison reveals that the balancing function as well as the ϕ_{rot}-method produce similar results. For low TIT the stator is more cooled than the rotor and thus both predicted mass flow rates are lower than the predicted values with a constant coolant split factor of 0.4. If the TIT rises the relative coolant consumption of the rotor grows and consequently also the required stage cooling air amount. It should be noted that the described trend is in line with Walsh estimation (see Fig. 3). In other words, for studies in a wide TIT range the split factor should be adapted and thus the usage of the split parameter ϕ_{rot} or the balancing function should be preferred.

4.2.2 Walsh

The Walsh method provides only one input parameter, the technology factor ϕ. This parameter varies the needed coolant mass flow rate for the stator and rotor independently. As a result, a parametric study with the described performance model would not lead to new findings, the results only reflect Fig. 3.

4.2.3 Horlock

For the Horlock cooling air estimation, the main input parameters are the variable C, the film cooling effectiveness ε_f, the cooling efficiency η_c and the maximum allowable blade temperature T_b. It should be noted that no detailed analysis for the variable C is carried out due to the linear influence of the cooling mass flow rate. For the remaining parameters, the influence has been evaluated by parameter studies and the results are presented graphically. In the corresponding graphs, the parameter influence on the cooling air consumption is shown for different inlet temperatures, whereby uncolored areas represent cooling air ratios of zero (uncooled) or above one (no core flow remaining). In these plots the vertical dashed lines mark the allowable blade temperature of 1250 K.

In Fig. 8 the influence of the cooling efficiency is shown. It can be seen that the cooling efficiency has an impact on the TIT at which the model predicts a cooling mass flow rate above zero. It should be noted that there is a mismatch between the TIT and the given maximum blade temperature of 1250 K. The estimated blade temperature at which the cooling flow starts approximates the given maximum allowable blade temperature with increasing cooling efficiency. This phenomenon is a result of the constant film cooling efficiency that also estimates a film cooling effect for a zero mass flow rate. With an increasing cooling efficiency this failure is reduced due to the higher coolant outlet temperature which lowers the film cooling effect. In the borderline case with a cooling efficiency of one the coolant outlet temperature equals the blade temperature and thus the surrounded gas temperature.

In Fig. 9 the variation of the cooling effectiveness is shown for a constant cooling efficiency η_c. The trend of the cooling air ratio does not present an unexpected behavior. The needed cooling air is monotonous increasing with rising TIT and with falling cooling effectiveness. Moreover, the same offset between maximum allowable blade temperature and the TIT can be observed as in Fig. 8. Only with a

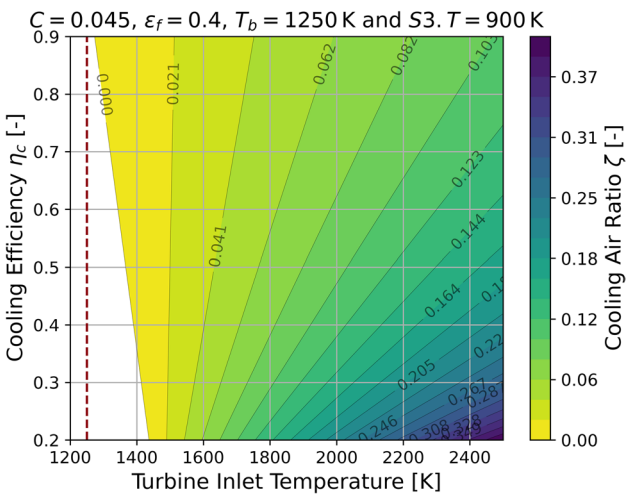

Fig. 8 Horlock predicted cooling air ratios ζ for different cooling efficiencies η_c and TIT

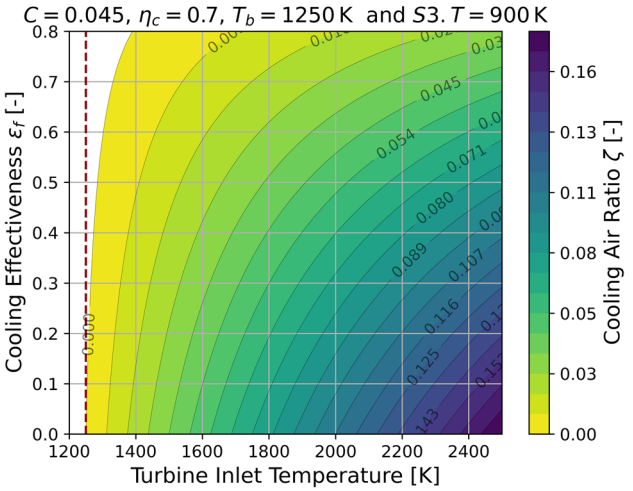

Fig. 9 Horlock predicted cooling air ratios ζ for different cooling effectiveness ε_f and TIT

cooling efficiency of zero the required coolant mass flow increases when the gas temperature exceeds the given blade temperature.

The offset between blade temperature and TIT can also be seen in Fig. 10 in which the influence of the maximum allowable blade temperature is shown. In addition, the figure shows that for a constant blade temperature, the cooling air ratio does not change for different TIT ranges. For example, with a blade temperature of 1250 K the cooling air ratio rises:

- from $\zeta = 0.9\%$ to 3.1% for a TIT change from 1400 to 1600 K
- from $\zeta = 9.7\%$ to 11.9% for a TIT change from 2200 to 2400 K

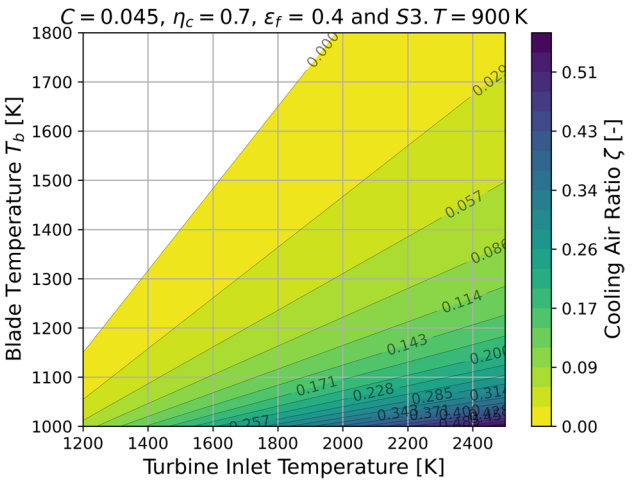

Fig. 10 Horlock predicted cooling air ratios ζ for different blade temperatures T_b and TIT

The parametric studies have shown, that the Horlock method should not be used for wide design range studies with constant design parameters. The constant parameter would lead to the discussed offset between the allowable blade and turbine inlet temperature. For an unrestricted use of the Horlock method, the cooling effectiveness and cooling efficiency would have to be provided in dependency of the current cooling air ratio.

4.2.4 Jonsson

The Jonsson method provides three parameters for calibration: the factor b, the exponent s and the allowable blade temperature T_b. For these Jonsson parameters, the same analyses are carried out as for the Horlock method.

Fig. 11 shows the influence of the b parameter of the cooling air ratio for film-cooled stages with an exponent $s = 1.5$. The required cooling air increases linear with the b parameter and disproportional with increasing TIT due to the selected Jonsson exponent ($s \neq 1.0$). It should also be noted that the averaged suggested parameters for film-cooled blades in table 1 lead to plausible cooling air ratios:

- one stage: $b = 0.075$ and $TIT = 1700\,K \Rightarrow \zeta = 12.0\%$
- two stages: $b = 0.15$ and $TIT = 1700\,K \Rightarrow \zeta = 24.0\%$
- stator: $b = 0.06$ and $TIT = 1700\,K \Rightarrow \zeta = 9.6\%$
- rotor: $b = 0.05$ and $TIT = 1650\,K \Rightarrow \zeta = 6.7\%$

The influence of the s parameter is shown in Fig. 12. While a TIT rise leads to a monotonous increasing cooling air demand, the s parameter trend changes at the point at which the term $\frac{TIT - T_b}{T_b - T_c}$ becomes one (vertical line). If the term

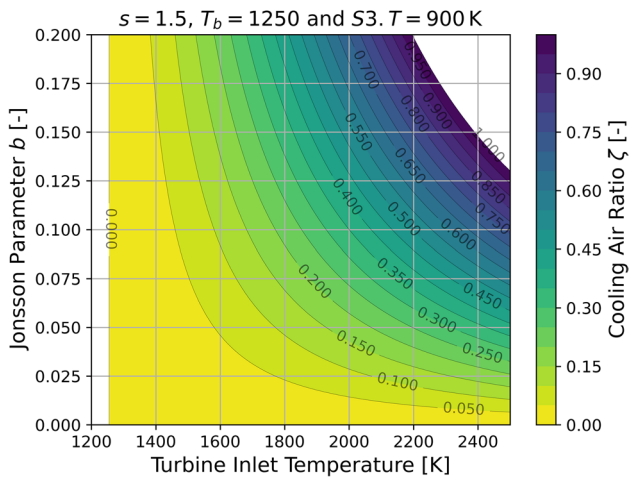

Fig. 11 Jonsson predicted cooling air ratios ζ for different Jonsson parameters b and TIT

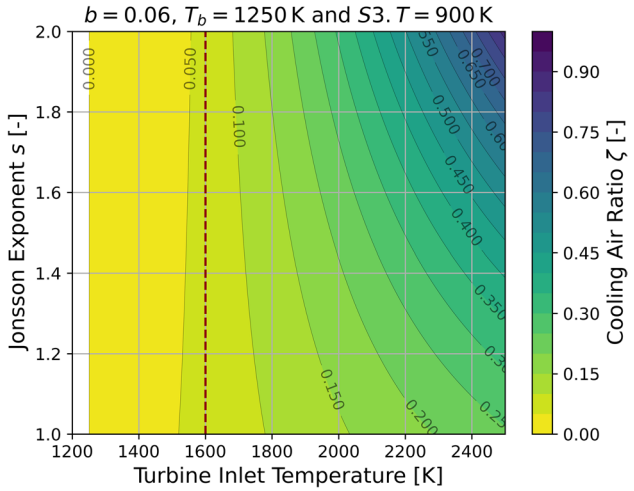

Fig. 12 Jonsson predicted cooling air ratios ζ for different Jonsson exponents s and TIT

is greater than one a higher exponent s leads to an increased cooling mass flow rate prediction. If the term sinks below one, the reverse trend can be observed. This means that the Jonsson exponent s not only influences the amount of cooling air but also defines how much the cooling air mass flow rate changes with temperature variations. Consequently, the parameter cannot be regarded as a technology factor.

Figure 13 shows the influence of the blade temperature on the estimated cooling air consumption. For the Jonsson method, the increase of the cooling mass flow rises with an increasing distance from the maximum allowable blade temperature:

- from $\zeta = 1.8\%$ to 6.5% for a TIT change from 1400 to 1600 K for $T_b = 1250\,\mathrm{K}$
- from $\zeta = 30.2\%$ to 40.5% for a TIT change from 2200 to 2400 K for $T_b = 1250\,\mathrm{K}$

4.2.5 Halliwell

The Halliwell requires only two design parameters: the technology factor C_1 and the blade temperature T_b. Due to the linear relation of C_1 in Eq. 12 the influence is not analyzed here.

Figure 14 shows the impact of the blade temperature and the TIT on the estimated cooling mass flow rate. In this plot, the same trend can be observed as for the Horlock method: the distance to the maximum allowable blade temperature has no influence on the growth of the cooling air consumption.

- from $\zeta = 2.1\%$ to 5.0% for a TIT change from 1400 to 1600 K
- from $\zeta = 13.5\%$ to 16.4% for a TIT change from 2200 to 2400 K

It should also be noted that the calculation of the Halliwell method basically corresponds to the Horlock method. The Halliwell C_1 parameter equals the Horlock K value for convective cooled blade (see Eq. 7 and Eq. 12). But the Horlock method uses an extended equation for film-cooled blades (see Eq. 9), in which additional parameters are considered. In Eq. 21 a direct comparison of the formulas is carried out and shows that for a constant cooling efficiency and a constant film cooling effectiveness the additional parameters can be summarized into one variable that allows a conversion between the C_1 and the K parameter. For example, the suggested Horlock values for the cooling efficiency $\eta_c = 0.7$ and the film cooling effectiveness $\varepsilon_f = 0.4$ leading to an overall cooling effectiveness ε_0 range between 0.5 and

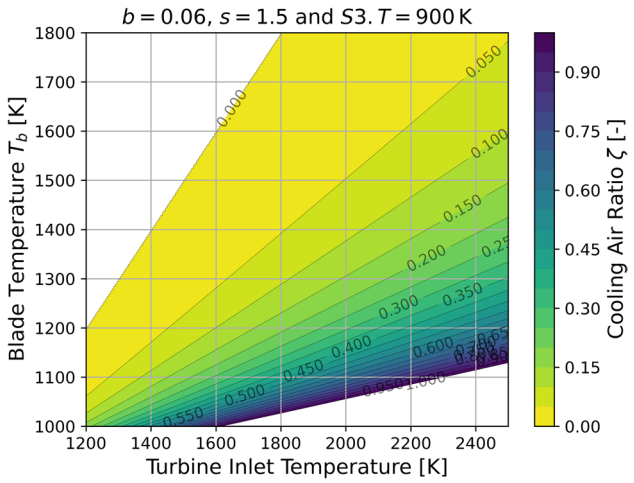

Fig. 13 Jonsson predicted cooling air ratios ζ for different allowable blade temperatures T_b and TIT

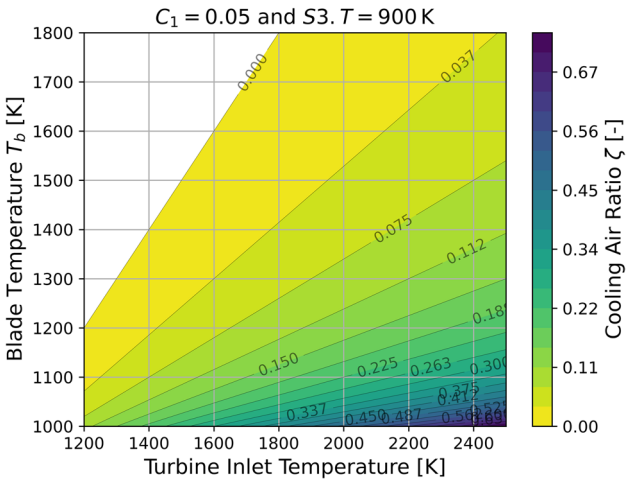

Fig. 14 Halliwell predicted cooling air ratios ζ for different blade temperatures T_b and TIT

0.7 to a variation of the factor f_{h-h} between 0.724 and 0.549. In other words, for film-cooled blades the Halliwell method predicts higher cooling air mass flow rates or blade temperatures if the recommended parameter of $C_1 = 0.05$ is used.

$$\overbrace{\underbrace{\zeta = \frac{K \cdot \varepsilon_0}{1-\varepsilon_0}}_{\widehat{=}\,\text{Halliwell}} \cdot \underbrace{\frac{1+\varepsilon_f \cdot \frac{(\eta_c - 1)}{\varepsilon_0} - \varepsilon_f \cdot \eta_c}{(1-\eta_c)} \cdot (1-\varepsilon_0)}_{f \text{ calculated with } \eta_c=0.7 \text{ and } \varepsilon_f=0.4}}^{\widehat{=}\,\text{Horlock}} \quad (21)$$

$$\Rightarrow C_1 = K \cdot f = \frac{C \cdot f}{\eta_c}$$

The Eq. 21 also allows to estimate the influence on the C_1 value using the Horlock for the calculation of cooling effectiveness ε_0 for different cooling air ratios. With ε_0 the C_1 value is determined by multiply K with the related factor f. Table 4 shows the results for different cooling ratios. It can be seen that the suggested value of $C_1 = 0.05$ matches well for cooling air ratios up to 6%. For higher ratios the C_1 parameter decreases.

4.3 Comparative Study

For a direct comparison of the methods presented, a comparative study has been carried out, which is now presented. Therefore, the cooling mass flow rate is evaluated with the Grieb method for different TIT by using the balance function to determine the cooling air split factor within the turbine stage. The cooling mass flow rates were then used to calculate the blade temperatures with the row-based methods. For this, the suggested default parameters were consistently used. In this process, the blade temperatures for the Grieb design point are calculated that equals MTO at sea level static by using the international standard atmosphere. Due to the strongly deviating design point of the Walsh method, this correlation is not considered in the comparison. The results are shown in Fig. 15, whereby the Grieb method predicts cooling mass flow rate from TIT = 950 K on. With increasing TIT, the differences between the predicted blade temperatures are increasing. In general, the Jonsson method estimates higher temperatures as the Halliwell method and the Halliwell method higher temperatures as the Horlock method. It should be noted that the required cooling air mass flow rate would also be predicted in the same order,

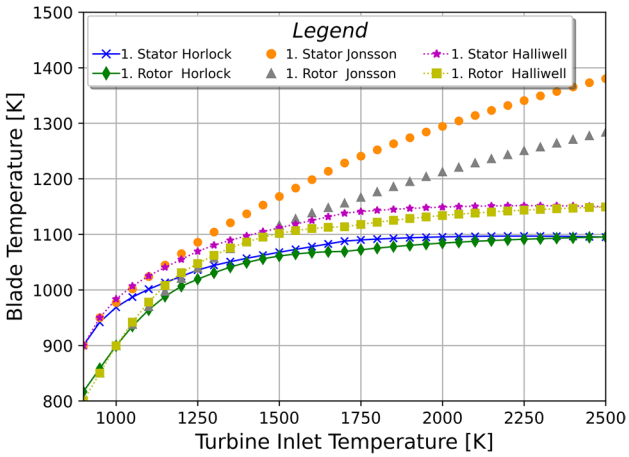

Fig. 15 Estimated blade temperatures for the predicted Grieb cooling air mass flow rates

if the blade temperature were specified. It should also be highlighted, that the predicted Halliwell and Horlock blade temperatures are relatively stable for TIT over 1500 K which shows that the methods predict a similar trend as the Grieb method. Moreover, the temperatures for stator and rotor are almost identical. This similarity is also influenced by the chosen temperature offset between rotor and stator which is currently set to -100 K. In contrast, the Jonsson method predicts for rising TIT also increased blade temperatures with a rotor-stator temperature difference of around 100 K. At that point, it should be noted that a change of the Jonsson exponent s can be used to influence the blade temperature increase. But the current available data does not allow to rate the shown trends and thus adjusting the parameter will not necessarily improve the predictions.

The estimated blade temperatures point out that the maximum allowable blade temperature T_b does not describe the surface temperature. A comparison between the predicted blade temperatures with allowable material temperatures from literature [12, 17] indicates that this parameter represents the base material temperature (under-coating layers). This assumption was also made, for example, in [18].

4.4 Calibration

In this section, the cooling air methods are calibrated to NASA's Energy Efficient Engine (EEE) [9, 19]. The considered one staged high-pressure turbine is film cooled and

Table 4 Results from Halliwell-Horlock matching process

ζ	[%]	2	4	6	8	10
ε_0	[%]	29.6	42.6	55.6	68.5	81.5
f	[-]	0.74	0.84	0.75	0.57	0.35
C_1	[-]	0.048	0.054	0.048	0.037	0.023

was designed by Pratt and Whitney. During the calibration process the technology factors of the cooling air methods were varied until the blade temperatures match to the documented averaged surface temperatures: a stator temperature of $T_{b-stat} = 1352.95\,\mathrm{K}$ and a rotor temperature of $T_{b-rot} = 1263.5\,\mathrm{K}$.

For the calculation, the described model from Sect. 4.1 is used in combination with the boundary conditions that are adapted or derived from the reports [9, 19]. The finally chosen boundary conditions are summarized in Table 5. In this table two coolant mass flow rates are given, the entries that are marked with *All* equal the sum of all reported cooling streams of the high-pressure turbine and the mass flow rates that are marked with *Airfoil* consider only the coolant streams which are ejected through the blades. For the Grieb method, the stator and rotor mass flow rate are combined and the fluid properties from stator cooling air are used. In the lower part of the table, the values for the CR are shown which are necessary for the Walsh cooling air estimation. It should also be noticed that the cooling air mass flow rate ratio is held constantly for the two operating points. According to [5], this assumption should not lead to significant errors.

Beside the two possible mass flow rates, the matching process is carried out for a rotor temperature offset of zero and – 224.1 K (see Sect. 3.6 and Eq. 22).

$$\Delta T_{MTO} = \underbrace{-204.1\,\mathrm{K} \cdot \left(\frac{231.1}{220.5}\right)^2}_{\text{derived from [9]}} = -224.1\,\mathrm{K} \tag{22}$$

Table 5 Boundary conditions for the EEE calibration

Position	Parameter	Unit	Value
MTO			
4	Mass Flow	[kg/s]	59.49
	Temperature	[K]	1708.15
Cooling Air Stator	Mass Flow (All)	kg/s	5.8934
	Mass Flow (Airfoil)	[kg/s]	4.3823
	Temperature	[K]	850.15
Cooling Air Rotor	Mass Flow (All)	kg/s	3.5278
	Mass Flow (Airfoil)	[kg/s]	1.8802
	Temperature	[K]	829.15
CR (Walsh)			
4	Mass Flow	[kg/s]	27.2069
	Temperature	[K]	1633
Engine	Mass Flow	[kg/s]	241.0779
Cooling Air	Mass Flow (All)	[kg/s]	4.3087
	Mass Flow (Airfoil)	[kg/s]	2.8641
	Temperature	[K]	760.28

In perspective, the results with an offset temperature of zero can be applied for thermodynamic simulations in which no assumptions are made about the temperature drop.

Table 6 shows which technology parameter has to be applied to match the cooling air mass flow rates of the EEE.

If the Grieb method is used with a high technology factor, the values of the case *all cooling air streams* can be assumed well. The computed $\phi = -0.1147$ seems reasonable for the EEE engine because the method considers engines with an entry into service until the year 2000 and the EEE is a test turbine that report was published in 1982. Hence, a fictive entry into service could be at the end of the considered timeline. In contrast, the ϕ value for the *airfoil cooling streams* seems too low. This finding corresponds with the documentation of the method in [4]. The necessary Walsh technology factors are far outside of the borders for both cases, the method overestimates the cooling air consumption for EEE.

For the row-based methods the stator parameters are above the expected area for all considered cases (see Sect. 3). In contrast, the determined rotor parameters are more in line with the suggested ranges. The best parameter match can be found for the case $\Delta T_{MTO} = 0\,\mathrm{K}$ and using *all cooling streams*.

At this point, it should be noted that the main difference between the stator and the rotor row parameter computation are the assumed blade temperatures. As a result, the calibration process is carried out with a common literature blade temperature of 1250 K for both rows [4, 12, 20] without a stagnation temperature offset for the rotor. The resulting parameters are presented in Table 7. It can be seen that the parameters are closer to the expected ranges.

The presented results cannot be used to derive a general statement of the methods quality or the best parameter choice. But it can be seen that the row-based methods would already provide a good assumption of the needed cooling air at an early design state by using the default parameter with an allowable blade temperature of 1250 K. If more detailed information about the turbine is available, the technology factors must be adapted to the corresponding case (see Table 6).

4.5 Application

For established engine concepts the empirical models can be used to determine the design cooling air mass flow rate with little computational effort. The thermal conditions in off-design operating points can be checked using the blade temperature predictions of the semi-empirical approaches. If the temperatures rise above the values that are calculated for the most stressed operating point (usually MTO) or the predicted temperatures seem too high, then these are indicators that the cooling air rates may need to be adjusted. For novel or less common engine concepts the usage of

Table 6 Calibrated technology factors

All cooling streams					
Mean	Parameter			Value	
Grieb	ϕ	[-]		– 0.1147	
Walsh	ϕ	[-]		– 1.8201	
Mean	Parameter		Stator	Rotor	
	ΔT_{MTO}	[K]	0	0	– 224.1
Horlock	C	[-]	0.1521	0.0514	0.2914
Jonsson	b	[-]	0.1518	0.0619	0.2475
Halliwell	C_1	[-]	0.1402	0.0627	0.1568
Airfoil cooling streams					
Mean	Parameter			Value	
Grieb	ϕ	[-]		– 0.9140	
Walsh	ϕ	[-]		– 2.1004	
Mean	Parameter		Stator	Rotor	
	ΔT_{MTO}	[K]	0	0	– 224.1
Horlock	C	[-]	0.1131	0.0327	0.1249
Jonsson	b	[-]	0.1129	0.0315	0.1146
Halliwell	C_1	[-]	0.1043	0.0327	0.0768

Table 7 Calibrated technology factors for a maximum allowable blade temperature of 1250 K

All Cooling Streams $\boldsymbol{\Delta T_{MTO} = 0\,K}$				
Mean	Parameter		Stator	Rotor
Horlock	C	[-]	0.0815	0.0583
Jonsson	b	[-]	0.0734	0.0559
Halliwell	C_1	[-]	0.0865	0.0587

the semi-empirical methods is recommended. As a first step, the most thermal stressed operating points should be identified by the predicted temperatures with initial cooling air design. Afterwards the requested permissible metal temperatures can be achieved by changing the cooling air ratio at the design operating point. In the case of major changes, the thermal stress should be rechecked for all important operating points in order to identify side effects of the cooling air design adjustments.

The correct choice of the technology factors for the considered cooling air methods is still challenging task. If reference data is available for a similar engine, a calibration of the technology factors should be preferred. If there is no further information available, the technology factors can be estimated on the basis of the analyses shown in Sect. 4.2 and values presented for the EEE in Sect. 4.4.

5 Conclusion and outlook

In this paper, five selected cooling air estimation methods from the literature were presented. Then all the steps required to implement the considered methods on the base of thermodynamic results were described. For the empirical Grieb method a new approach has been developed which allows to split the stage coolant mass flow to the stator and rotor without defining a second design parameter, thus applicability and repeatability could be improved. In addition, an approach for more detailed analyses was introduced that estimates the stagnation temperature drop between the stator and rotor, which improves the blade temperature estimation for off-design considerations. Moreover, a newly developed method was presented that allows the cooling air prediction for unlimited turbine stages.

In Sect. 4 the extended performance code was used to investigate the influence of the main parameter of the different cooling air methods. Additionally, a comparison of the methods was carried out and the main parameter were calibrated using the public EEE data.

In general, the empirical methods from Grieb and Walsh are more robust than the row-based methods and differ mainly by the specified design operating point. The statistical databases of both methods cannot deliver good estimation for unusual or novel engine concepts, nor for innovative airplane designs. As an example, for an ultra-high bypass engine the most stressed operating point can

move from maximum take-off to top of climb. Such a change in the critical operating point cannot be considered by both empirical approaches. However, a comparison of the two empirical methods leads to the conclusion that the Grieb method appears more attractive due to the transparent data base and the better agreement with the EEE.

In contrast to the fully empirical approaches the semi-empirical methods are not fixed on a specified design operating point and thus a change of the critical operating point does not limit the application. Furthermore, improvements in material or blade cooling technology could be considered. However, the main advantage is that the blade temperatures can be estimated which allows first estimations of blade lifetime. Which of the semi-empirical methods should be used is highly dependent on the available turbine information. For the case that only thermodynamic assumptions are available the Jonsson or the Halliwell method is a good choice. If detailed information about the blade cooling is available, the Horlock method provides several parameters to improve the level of detail. To enhance the off-design blade temperature predictions in general, the semi-empirical methods can be combined with the presented temperature offset estimation.

Another important point in determining cooling air consumption is the choice of the design parameters, which has an impact on the results for all cooling methods. The calibration of the considered approaches in Sect. 4.4 had exposed that the design parameter should be chosen in relation to the used information. Therefore, parameter sets were presented for different use cases. It was also shown that the semi-empirical cooling air methods can estimate the cooling air consumption of the EEE well, if the default parameters from the literature are used. Therefore, the reference blade temperature must be set to the base material temperature and the temperature offset between absolute (stator) and relative system (rotor) should not be considered.

In future, the determination of required cooling air with the semi-empirical methods could be further improved by the utilization of a lifetime estimation for the turbine blades. Such a process would allow an improved cooling air calculation by considering the lifetime of a representative mission. For example, engines with different bypass ratios could be designed with the constrain that the applied coolant mass flow rates result in the same lifetime reduction for the assumed flight mission, whereby the sizing effects on the component efficiencies should also be taken into account.

Author Contributions B.S. carried out literature research, the conception of the work, the studies and the interpretation of data (sole author)

Funding Open Access funding enabled and organized by Projekt DEAL.

Data Availability No datasets were generated or analysed during the current study.

Declarations

Conflict of interest The authors declare no Conflict of interest.

References

1. Horlock, J.H.: Advanced Gas Turbine Cycles. Pergamon, Oxford (2003). ISBN: 978-0-08-044273-0
2. Jonsson, M., Bolland, O., Bücker, D., Rost, M.: Gas turbine cooling model for evaluation of novel cycles. Proceedings of ECOS 2005 (2005)
3. Kurzke, J.: Preliminary design; aero-engine design: A state of the art. vki lecture series (2013)
4. Grieb, H.: Projektierung von Turboflugtriebwerken Technik der Turboflugtriebwerke. Birkhäuser, Basel, Schweiz (2004). https://doi.org/10.1007/978-3-0348-7938-5. ISBN: 978-3-0348-9627-6
5. Walsh, P.P., Fletcher, P.: Gas Turbine Performance, 2nd edn. Blackwell Science, Oxford (2004). ISBN: 0-632-06434-X
6. Becker, R.-G., Wolters, F., Otten, T., Nauroz, M.: Development of a gas turbine performance code and its application to preliminary design. Deutscher Luft- und Raumfahrtkongress DLRK (2011)
7. Schneider, B.: Virtualization of the DLR Turbine Test Facility NG-Turb. Deutscher Luft- und Raumfahrtkongress DLRK (2020). https://doi.org/10.25967/530132
8. Schneider, B.: Transient Thermodynamic Simulation of the DLR Turbine Test Facility NG-Turb. AIAA SciTech Forum (2023). https://doi.org/10.2514/6.2023-2521
9. Thulin, R. D., Howeand, D. C., Singe, I.D.: Energy Efficient Engine - high-pressure turbine detailed design report. NASA contractor report (1982)
10. Kurzke, J., Halliwell, I.: Propulsion and Power. Springer International Publishing, Cham (2018). https://doi.org/10.1007/978-3-319-75979-1. ISBN: 978-3-319-75977-7
11. Horlock, J. H., Watson, D. T., Jones, T. V.: Limitations on gas turbine performance imposed by large turbine cooling flows. Journal of Engineering for Gas Turbines and Power (2001). https://doi.org/10.1115/1.1373398. ISSN: 0742-4795.
12. Yin, F., Tiemstra, F. S., Rao, A. G.: Development of a flexible turbine cooling prediction tool for preliminary design of gas turbines. J Eng Gas Turbines Power (2018). https://doi.org/10.1115/1.4039732. ISSN: 0742-4795
13. Bräunling, W. J. G.: Flugzeugtriebwerke: Grundlagen, Aero-Thermodynamik, ideale und reale Kreisprozesse, thermische Turbomaschinen, Komponenten, Emissionen und Systeme 3., vollst. überarb. und erw. aufl. edn. VDI-Buch (Springer, Berlin, 2009). ISBN: 978-3-540-76368-0

14. Cumpsty, N. A.: Jet propulsion: A simple guide to the aerodynamics and thermodynamic design and performance of jet engines, 2nd edn. Cambridge University Press, New York (2003). ISBN: 0521541441
15. Krumme, A.: Konzeption. KOBRA Dokumentenserver der Universität Kassel, Implementierung und Anwendung eines automatisierten aerothermodynamischen Vorentwurfsprozesses für Axialturbinen (2016)
16. Becker, R.-G., Bolemant, M., Krause, D., Peitsch, D.: An automated process to create start values for gas turbine performance simulations using neuronal networks and evolutionary algorithms. International Gas Turbine Congress (2015)
17. Benini, E.: Advances in gas turbine technology. InTech, Rijeka (2011). ISBN: 978-953-307-611-9
18. Young, J.B., Wilcock, R.C.: Modeling the air-cooled gas turbine: Part 2 - coolant flows and losses. J. Turbomach. **124**, 214–221 (2002). https://doi.org/10.1115/1.1415038
19. Halle, J. E., Michael, C. J.: Energy efficient engine fan component detailed design report
20. Woelki, D., Peitsch, D.: Modeling and potentials of flexible secondary air systems regarding mission fuel burn reduction and blade creep live. ISABE-2019-24435 (2019)